

**ROTORCRAFT BLADE/VORTEX INTERACTION NOISE:
ITS GENERATION, RADIATION, AND CONTROL**

J. S. Preisser* , T. F. Brooks** , and R. M. Martin†
NASA Langley Research Center
Hampton, Virginia 23665

Abstract

Recent results are presented from several research efforts aimed at the understanding of rotorcraft blade-vortex interaction noise generation, directivity, and control. The results are based on work performed by researchers at the NASA Langley Research Center, both alone and in collaboration with other research organizations. Based on analysis of a simplified physical model, the critical parameters controlling the noise generation are identified. Detailed mapping of the acoustic radiation field reveals the extreme sensitivity of directivity to rotor advance ratio and disk attitude. A means of controlling blade-vortex interaction noise by higher harmonic pitch control is discussed.

Introduction

Blade/vortex interaction (BVI) noise, due to rotor blade interaction with shed tip vortices of preceding blades, has been a major topic of rotorcraft acoustic research for the past several years. BVI noise is intense, impulsive, and has frequency content in the mid-frequency, audible range making it one of the most objectionable types of rotorcraft noise. Moreover, it is most likely to occur during low speed rotorcraft descent, such as during approach for landing at heliports, which are often located in areas of high population.

The literature pertaining to BVI noise is broad and has involved many researchers from various organizations. Much of the work has been experimental. A comprehensive theory, able to accurately predict BVI generation and radiation for full-scale rotorcraft, is not yet available. Past experimental work in rotor BVI noise has attempted to define the operating regimes for its occurrence and the general direction of its radiation, utilizing both flight measurements¹⁻³ and wind tunnel tests.⁴⁻⁶ BVI has been found to be most intense forward of the advancing side of the rotor and down from the plane of the rotor.¹ Further experimental

results have indicated that, the more nearly parallel the tip vortex is to the blade at the time of interaction, the more intense is the noise.⁷ These previous tests were unfortunately limited by a small number of fixed measurement locations. Questions remained as to the sensitivity of radiation direction with changing advance ratio and tip-path plane angle, as well as to its controllability.

The present paper presents results from recent contributions by researchers at NASA Langley Research Center to the understanding of BVI noise generation⁸, radiation^{9,10}, and control.¹¹ The experimental part of the research was conducted in collaboration with personnel from the Aerostructures Directorate, U.S. Army ARTA, AVSCOM,^{9,11} and the German Aerospace Research Establishment, DLR.^{9,10} There is no intent in the present paper to assess the current state-of-the art in BVI. Instead, the paper focuses on results from a simplified physical analysis of the critical parameters controlling BVI, and results from tests conducted in the German-Dutch DNW wind tunnel and the Transonic Dynamics Tunnel (TDT) at NASA Langley. The former test provided the first comprehensive set of data on BVI directional characteristics as a function of rotor advance ratio and disk attitude. The latter examined the effectiveness of higher harmonic pitch control for BVI noise reduction.

Blade-Vortex Interaction Noise Generation

Rotorcraft blade-vortex interaction (BVI) is a highly complex, three-dimensional, time dependent phenomena. As the rotor blades rotate, vorticity is continuously shed from the tip of each blade, due to the pressure difference between the upper and lower surfaces of each lifting blade. The vorticity rapidly rolls up in the preferred direction generating spiraling tip vortices whose paths depend on the rotational speed of the rotor, the forward speed of the rotorcraft, and the orientation of the rotor disk plane to the flight direction. In general, the vortex path is downward away from the rotor plane because of the rotor downflow, and thus does not ordinarily interact strongly with the rotor blades. However, under certain operating conditions, such as during rotor descent at slow forward speed, the tip vortex paths intersect the rotor disk plane, generating impulsive loading to the blade, which results in noise. A

* Head, Aeroacoustics Branch, Acoustics Division. Associate Fellow AIAA

** Senior Research Scientist, Aeroacoustics Branch, Acoustics Division

† Research Scientist, Aeroacoustics Branch, Acoustics Division. Associate Member AIAA.

schematic illustrating the complexity of the blade vortex interaction process for a 4-bladed rotor system is shown in Figure 1. The blade on the advancing (right hand) side of the figure depicts multiple interactions due to the tip vortices of the blades 180 and 270 degrees ahead. This situation is typical for moderate to high rotorcraft forward speeds. Lower speeds would produce more interactions due to the increased number of vortices present in the rotor plane. The blade near the top of the figure illustrates an interaction nearly normal to the blade due to the tip vortex of the preceding blade, although such normal interactions are apparently not important to the BVI noise production. A retreating (left hand) side BVI is also evident.

As mentioned previously, a rigorous prediction of the BVI noise generating phenomena is not yet possible. However, advances are being made in numerical simulations of BVI noise. Reference 12 discusses some of the more recent methods. Nevertheless, much can be understood about BVI from simple models. For example, based on analysis of a simplified two-dimensional, shock-free physical model, Hardin and Lamkin⁸ have found the controlling parameters for BVI noise to be the following: (1) the incoming vortex circulation strength, Γ ; (2) the portion of the blade span over which two-dimensional (parallel) interaction occurs, ℓ ; (3) the vortex miss distance, r ; and (4) the lift, L , on the blade at the time of the interaction. Figure 2 presents a simple schematic diagram illustrating these parameters during a single interaction. The figure shows a near parallel interaction with the vortex passing beneath the blade. A typical BVI noise signature resulting from a single such interaction for an observer position below the rotor plane was calculated and is presented in Figure 3. Note that the signature consists of a positive peak followed by a somewhat larger negative peak. As will be shown later in this paper, the effects of multiple interactions produce a much different signature in the farfield. Although the calculated result from such a simplified analysis cannot predict the measured result, the physical insight derived from such an analysis has proven useful in both explaining the trends of BVI far-field directivity as well as suggesting means for its control. BVI noise directional characteristics and BVI noise control are the topics of the remaining parts of this paper.

Blade-Vortex Interaction Noise Directional Characteristics

The following results are taken from References 9 and 10, and are based on two rotor BVI experiments performed jointly with personnel of the German

Aerospace Research Establishment, DLR. The reader is referred to those works for a more detailed account.

Test Description

Wind Tunnel.- The tests were performed in separate entries in 1986 and 1988 in the open test section of the Duits-Nederlandse Wind Tunnel, DNW. The facility is a large, subsonic, atmospheric closed circuit tunnel with open and closed test sections and is located in the Northeast Polder, The Netherlands. The open configuration utilizes an 8x6 meter nozzle that provides a free jet to the test section, which is 19 meters in length and is surrounded by a large anechoic room of about 23,000 cubic meters with absorptive acoustic wedges. The maximum tunnel speed is about 80 m/s. The background noise levels are low, an ideal condition for aeroacoustic testing.

Model Rotor.- The rotor used in this research was a 40 percent, dynamically scaled model of a four-bladed, hingeless B0-105 main rotor. A photograph of the rotor mounted in the DNW open test section is presented in Figure 4. Details of the rotor test stand used to support the model as well as to house the hydraulic drive system, rotor balance system, and rotor control system may be found in Reference 9. The rotor has a diameter of 4 meters with a NACA 23012 airfoil cross-section. The nominal rotor operating speed was 1050 rpm, which resulted in an acoustic blade-passage-frequency of about 70 Hz. The nominal rotor tip speed was 218 m/s for a hover tip Mach number of 0.64.

Acoustic Instrumentation.- The acoustic instrumentation consisted of nine microphones placed in a linear array on a traversing system and two additional microphones mounted on the rotor fuselage. The nine-element array and traversing system can be seen in Figure 4. The array microphones were arranged symmetrically with respect to the tunnel centerline, spaced 0.54 m apart, 2.3 m below the rotor hub. The traversing system allowed movement of the microphones both upstream and downstream of the hub.

Data Analysis.- Utilizing a blade position reference (once-per revolution) signal, 40 rotor revolutions of the raw acoustic signals were digitized and then bandpass filtered to remove low frequency loading and thickness noise and high frequency broadband noise. This process resulted in acoustic time histories dominated by BVI noise in the mid-frequency range. To obtain directivity patterns, peak amplitude values were used for each microphone in the array for various array positions upstream and downstream of the rotor hub. This resulted in a directivity coverage corresponding to a plane beneath

the rotor (see Figure 5). The results were then corrected to account for effects of spherical spreading. Differences in assumed source locations on advancing and retreating sides of the rotor were taken into account as part of this analysis process.

Results and Discussions

Multiple BVI.- Bandpass (600 - 5000 Hz) filtered time histories of the nine-microphone array at five traverse locations are presented in Figure 6. The time histories correspond to one representative blade passage for an advance ratio μ of 0.115; a rotor tip-path-plane angle, α_{TPP} , of 3.4° ; at a thrust coefficient, C_T , of 0.0044. All measurements were upstream of the rotor hub and show three distinct impulsive events A, B, and C on the advancing side. The time histories were inspected to identify the peak amplitude and arrival time of each individual impulse over the entire measurement plane. Acoustic triangulation⁹ was used to estimate the locations of each of the three impulses on the rotor disk. The peak amplitudes in Pascals of each impulse were then normalized to a reference distance of 4 m. The resulting directivity patterns are shown in Figure 7.

Impulse A is the earliest detectable BVI impulse, and was found to occur at about a 55° rotor azimuth. This impulse has the lowest acoustic level and radiates a lobe forward and to the right of the projection of the rotor disk hub on the measurement plane. Impulse B, near 61° azimuth, shows higher acoustic levels and radiates more in a forward direction. Impulse C, created at 68° azimuth, has the highest noise levels and radiates nearly directly forward. These patterns suggest that the noise source's location on the rotor disk has an important effect on the resulting directivity pattern. Recall from Figure 1, that multiple BVI's can occur, and that the blade-vortex interaction angle is dependent on which vortex system is interacting. It has been shown in Reference 13 that in addition to local Mach number, blade-vortex angle affects BVI noise directionality. This may explain the shift in farfield BVI pattern with changing BVI location on the rotor disk.

Effect of Tip-Path-Plane Attitude.- This section presents data acquired during the 1988 model rotor B0-105 noise test in DNW.¹⁰ BVI directivity patterns based on filtered, averaged, root-mean-square sound pressure were determined for different advance ratios for a number of tip-path-plane angles. Figure 8 presents the variation of patterns with tip-path-plane angle at an advance ratio of 0.15. Two primary lobes are observed: one on the advancing side of the rotor, the other on the retreating side. The BVI lobe from the advancing side interactions starts with a moderate

level upstream of the rotor at $\alpha_{TPP} = 0.6^\circ$. As tip-path-plane angle increases such as for steep helicopter descent, the lobe moves to the right of the flight path, and the acoustic levels increase. The lobe finally moves off the measurement plate at $\alpha_{TPP} = 6.5^\circ$.

One of the aims of the present test was to acquire directivity data on retreating side BVI at locations further downstream than the earlier test.⁹ Unfortunately, the results given here show that the measurement locations were not far enough downwind to completely define the retreating side BVI radiation lobe. The maximum downwind location of the microphone array was limited by interference with the sting, and by the increasing proximity to the lower shear layer of the open jet test section. However, the patterns for the 0.15 advance ratio indicate that the retreating side downwind lobe intensity and directivity are very sensitive to changes in tip-path-plane angle. The levels of the retreating side BVI seem to be nearly as intense as that radiated from the advancing side. Retreating side BVI lobes were also evident in the patterns of the remaining test conditions but were not sufficiently defined to make more specific conclusions.

Source Locations.- Wake geometry predictions from the Scully free wake in CAMRAD/JA were used to estimate the most likely BVI regions, as explained in Reference 10. The results for $\alpha_{TPP} = 3.6^\circ$ and $\mu = 0.15$ are presented in Figure 9 along with the directivity contour plot from Figure 8. Symbols are used to differentiate between encounters with the tip vortices of the four different blades. The occurrences are not at the individual symbol locations shown but over finite regions encompassing clusters of symbols. The symbols placement in the plot is dependent on the 15° resolution limitation of CAMRAD with regard to both blade and vortex positioning. The sizes of the symbols are scaled with each vortex's vertical "miss distance," r (see Fig. 2) with the largest symbols being the closest interactions. The open symbols signify the vortex passing under the blade; the solid symbols signify those passing above the blade.

The primary advancing side interactions are probably due to vortex 1 (circles), vortex 3 (diamonds) and vortex 4 (triangles), all near the 60 azimuth line. Vortex 4 is passing from above to below the blades when it is near 60° azimuth, 80 percent radius. The primary acoustic radiation direction is considerably to the right of the flight path for this flight condition, and is roughly normal to the 50° or 60° azimuth line. The high acoustic levels may be due to the fact that the interactions are

occurring near the tip where the local Mach number is high.

The strongest retreating side BVI is due to vortex 1 (circles), near 300° azimuth, 80 percent radius. Moderate BVI acoustic levels are measured under the aft retreating side of the rotor, in a direction approximately normal to 300° azimuth.

The free wake calculations were used to estimate the interaction locations for test conditions at several other advance ratios, with consistent correlation between the general azimuthal location of the strongest interactions and the general direction of the strongest acoustic radiation. The wake geometry results show that increasing rotor disk angle causes the general region of BVI to move downstream on the rotor disk, causing the interactions to occur at earlier azimuth angles, and therefore causing the noise to radiate more to the right and downstream of the rotor flight path. The comparison of the BVI location regions with the acoustic directivity patterns clearly supports the conclusion that the BVI noise source radiates most strongly in a direction roughly normal to the blade span.

Blade-Vortex Interaction Noise Control

The following results are based on a test performed in the NASA Langley Transonic Dynamics Tunnel on the subject of BVI noise control. Details of the experiment may be found in Reference 11.

Test Description

Wind Tunnel. The Transonic Dynamics Tunnel at Langley is a closed circuit, hard-walled, wind tunnel with a 16 ft square test section. Either air or Freon-12 can be used as the test medium. The latter was used for this test since the model rotor was dynamically scaled for operating in this medium, and test Reynolds numbers were higher (closer to full-scale). Because of the freon medium, matched Mach number conditions are achieved with lower rotor and tunnel speeds.

Model Rotor. The test was conducted using the Aeroelastic Rotor Experimental System (ARES). A photograph of the model set-up in the wind tunnel is shown in Figure 10. The rotor had four blades and was 110 in. in diameter. Each blade had an untwisted NACA 0012 airfoil section with a 4.24 in. chord.

The model rotor was capable of higher harmonic pitch control in the following manner. Blade pitch motion is applied to the rotor through swashplate motions due to three hydraulic actuators. For this four-bladed rotor, the higher harmonic pitch is

achieved by superposition of 4/rev (4P) swashplate motion upon basic fixed swashplate collective and cyclic (1P) flight control inputs. Four/rev collective pitch motion is possible (all four blades pitching the same way simultaneously), as are pitch schedules containing 3P, 4P, and 5P pitch harmonic components, through proper phasing of the 4P inputs. For this test, a specially developed computer-based open-loop control system was used to superimpose the higher harmonic pitch signals on the ARES control system. The pitch motion achieved can be described with the aid of Fig. 11 which shows blade pitch angle data versus blade azimuth angle for a specific flight condition. The 4P higher harmonic pitch portion (obtained by subtraction of the total from the baseline case) is seen at the bottom of the figure. The net pitch is seen not to be purely a 4P collective, but contains other harmonics due to normally occurring pitch-flap and pitch-lag couplings. For the 4P collective noise data shown in this report, the higher harmonic collective pitch amplitude θ_c at azimuthal angle Ψ_c in the first quadrant ($0 < \Psi_c < 90^\circ$) is defined in the manner shown in Fig. 11. The test procedure for implementing higher harmonic pitch control is described in Reference 11.

Acoustic Instrumentation. Twelve one-quarter inch diameter B&K pressure type microphones were used to make noise measurements. The microphones were fitted with nose cones and mounted in vibration isolated streamlined microphone stands. A special calibration scheme was devised and a scaling analysis was made to address the issue of acoustic measurements in a test medium other than air.

Data Analysis. Because of the reverberant nature of the test section, directivity measurements would be contaminated by reflections. Hence, it was decided to use the microphone measurements to determine sound power.

The noise data presented here are from initial processing obtained on-line during the test from the three microphones indicated in Fig. 10. The microphone signals were analog band-pass-filtered between 200 to 1600 Hz (3 dB down at 4.5 and 37 blade passage harmonics) to emphasize the impulsive BVI dominated portion of the noise. The sound pressure levels for each microphone were averaged to obtain a single dB value for each test point. Although little meaning is attached to the absolute dB values for present purposes, the relative levels and trends should be representative of more detailed analyses.

Results and Discussion

The rotor was tested over a broad range of operating conditions where the rotor thrust coefficient C_T was maintained at 0.005. Rotor advance ratios μ less than 0.11 were not possible due to wind tunnel minimum operating speed limitations. The rotor rotational speed was 650 rpm (the hover tip Mach number was nominally 0.62). Specific test flight conditions were defined based on the tunnel referenced tip path plane angle α and the advance ratio μ at the specified C_T . Tip path angles were corrected to account for the closed wall wind tunnel effects. In order to interpret the noise results in terms of full scale flight conditions, equivalent flyover descent angles Θ were calculated based on fuselage-rotor drag of an MBB BO-105.

The concept underlying noise reduction by higher harmonic pitch control is illustrated in Fig. 12. Recall from an earlier discussion that BVI noise generation was found to increase with vortex strength and blade lift (which is proportional to blade pitch) at the time of interaction. It is quite apparent that pitch control would not only modify lift pitch but would also modify the strengths of the shed vortices as well as possibly the interaction locations. The amplitude and phasing of such pitch controls may be expected to be important to the noise problem, since as shown previously the strongest BVI occurrences tend to be located within a limited rotor azimuth angle range of the first rotor quadrant.

A key objective of the test was to define flight regimes for which higher harmonic pitch control can be used to reduce BVI noise. Figure 13 shows, for the baseline (no control) case, a contour map of noise levels for a broad range of "full scale helicopter" descent angles Θ and advance ratios μ . A contouring program was used with measured levels at the test grid points indicated.

Similar data were also obtained for a 4P pitch control of $\theta_c = -1^\circ$ and $\Psi_c = 60^\circ$. While this pitch is not always at optimum (as seen in Ref. 11) it appears to give representative noise reductions for flight conditions at which reductions were found. Figure 14 shows the contour plot for the resultant levels. The effect on the noise is dramatic since the particularly intensive BVI noise region at low advance ratio and high descent angle is eliminated. Figure 15 shows the relative change between the levels of Fig. 14 and that of Fig. 13. Noise reduction is seen to be limited to the landing approach flight regime where BVI noise is most important. The maximum net reduction found was 4.7 dB at $\Theta = 8.5^\circ$ and $\mu = .11$. When higher harmonic control is employed, noise tends to increase where BVI is not dominant; that is,

for climb, level flight, steep descent, and high speed flight for all angles. Thus, HHC should not be used in these regimes. As mentioned previously, the particular 4P pitch control amplitude and phase used is not always optimum. The overall results, nevertheless, are encouraging and suggest further research is warranted.

Concluding Remarks

Much progress has been made in the last few years on the understanding of blade-vortex interaction (BVI) noise generation, radiation, and control. Researchers at the NASA Langley Research Center both alone and in collaboration with other research groups have contributed to that understanding. Through a simple, two-dimensional analysis, noise generation was shown to depend on four parameters: the incoming vortex strength, the blade lift (pitch), the length over which the interaction occurs, and the blade-vortex miss distance. As a result of two major studies of BVI directivity in the DNW wind tunnel, BVI noise was found to be highly directional and extremely sensitive to rotor advance ratio and disk attitude. A rotor free wake analysis demonstrated the likelihood of multiple BVI's, as suggested by the measurements. In addition, the peak radiation direction was consistent with the simple analysis and interaction regions on the rotor disk as predicted by the wake analysis. Moreover, the knowledge gained through the analysis and wind tunnel results suggested a means of BVI noise control, namely higher harmonic pitch control. A test was subsequently performed in a hard-walled tunnel, which clearly demonstrated a sound power reduction was possible for rotorcraft operation conditions typical of landing approach. BVI noise reductions appeared to correspond to reductions in blade lift (pitch) and vortex strength in the vicinity of BVI encounters.

Much needed physical insight into BVI has been gained through this research. Further research, however, is required before BVI noise can be routinely and accurately predicted, and before BVI noise control can be optimized.

References

- ¹Boxwell, D. A. and Schmitz, F. H.: "Full-Scale Measurements of Blade Vortex Interaction Noise." J. Am. Helicopter Society, Vol. 27, No. 4, October 1982.
- ²Charles, B. D.: "Acoustic Effects of Rotor-Wake Interaction During Low-Power Descent." Presented at the American Helicopter Society Symposium on Helicopter Aerodynamic Efficiency, May 6-7, 1975.

³Tangler, J. L.: "Schlieren and Noise Studies of Rotors in Forward Flight." AHS Preprint No. 77.33-05, May 1977.

⁴Spletstoesser, W. R.; Schultz, K. J.; Boxwell, D. A.; and Schmitz, F. H.: "Helicopter Model Rotor-Blade Vortex Interaction Impulsive Noise: Scalability and Parametric Variations." NASA TM 86007, December 1984.

⁵Hoad, D. R.: "Helicopter Model Scale Results on Blade-Vortex Interaction Impulsive Noise as Affected by Tip Modification." Paper No. 80-62, 36th Annual Forum, American Helicopter Society, May 1980.

⁶Martin, R. M.; and Connor, A. B.: "Wind Tunnel Acoustic Results of Two Rotor Models with Several Tip Designs." NASA TM 87698, July 1986.

⁷Schlinker, R. H.; and Amiet, R. K.: Rotor Vortex Interaction Noise. NASA CR 3744, October 1983.

⁸Hardin, J. C. and Lamkin, S. L.: "Concepts for Reduction of Blade/Vortex Interaction Noise," J. Aircraft, Vol. 24, No. 2, February 1987, pp. 120-125.

⁹Martin, R. M.; Spletstoesser, W. R.; Elliott, J. W.; and Schultz, K. J.: "Advancing Side Directivity and Retreating Side Interactions of Model Rotor Blade Vortex Interaction Noise." NASA TP 2784, AVSCOM Technical Report 87-B-3, May 1988.

¹⁰Martin, R. M.; Marcolini, M. A.; Spletstoesser, W. R.; and Schultz, K. J.: Wake Geometry Effects on Rotor Blade-Vortex Interaction Noise Directivity, NASA TP-3015, 1990.

¹¹Brooks, T. F.; Booth, E. R. Jr. ; Jolly, J. R. Jr.; Yeager, W. T. Jr.; and Wilbur, M. L.: "Reduction of Blade-Vortex Interaction Noise Through Higher Harmonic Pitch Control," J. Am. Helicopter Society, Vol. 35, No. 1, January 1990, pp. 86-91.

¹²Hassan, A. A.; Tadghighi, H.; and Charles, B. D.: "Aerodynamics and Acoustics of Three-Dimensional Blade-Vortex Interactions." NASA CR 182026, 1990.

¹³Widnall, S.: "Helicopter Noise Due to Blade-Vortex Interaction," JASA, Vol. 50, No. 1, Part 2, 1971.

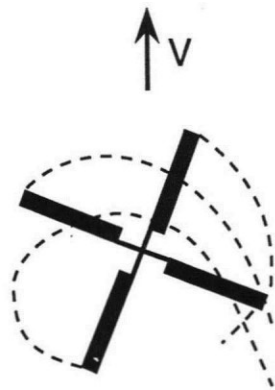


Figure 1. Blade and vortex positions in forward flight

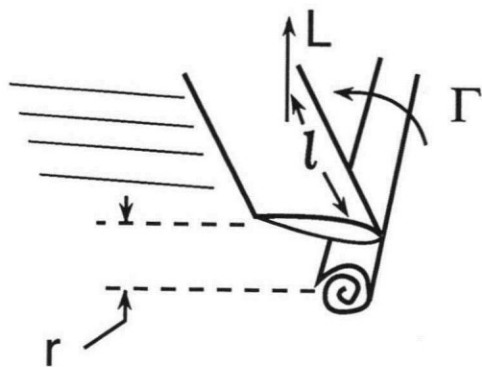


Figure 2. Schematic showing key parameters for BVI.

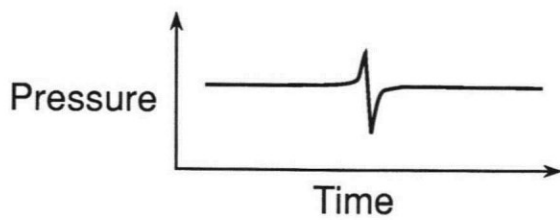


Figure 3. Calculated BVI noise signature.

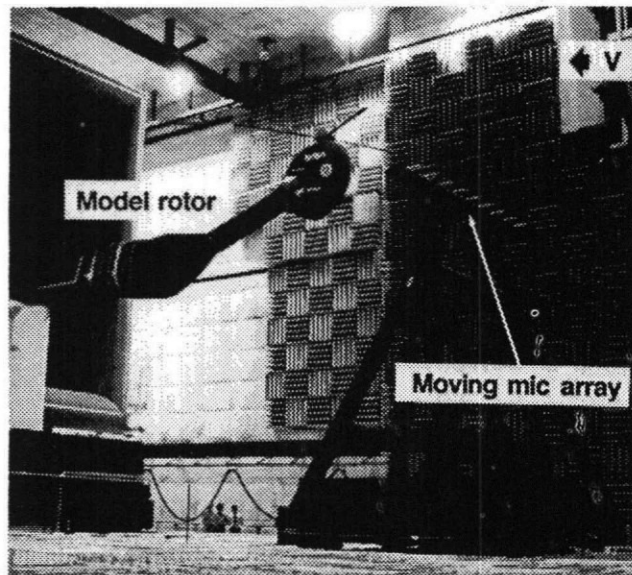


Figure 4. Photo of model rotor in DNW.

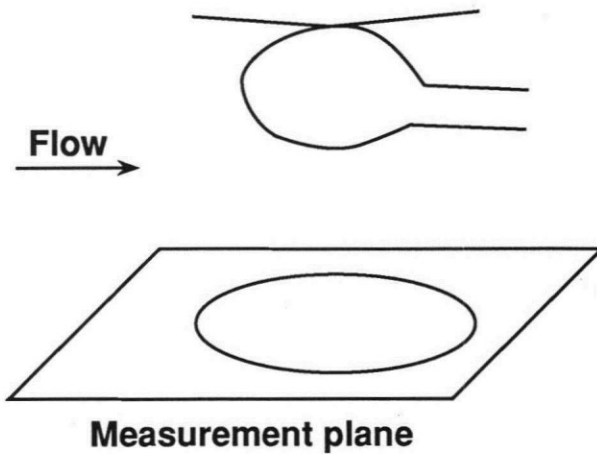


Figure 5. Sketch depicting acoustic measurement plane.

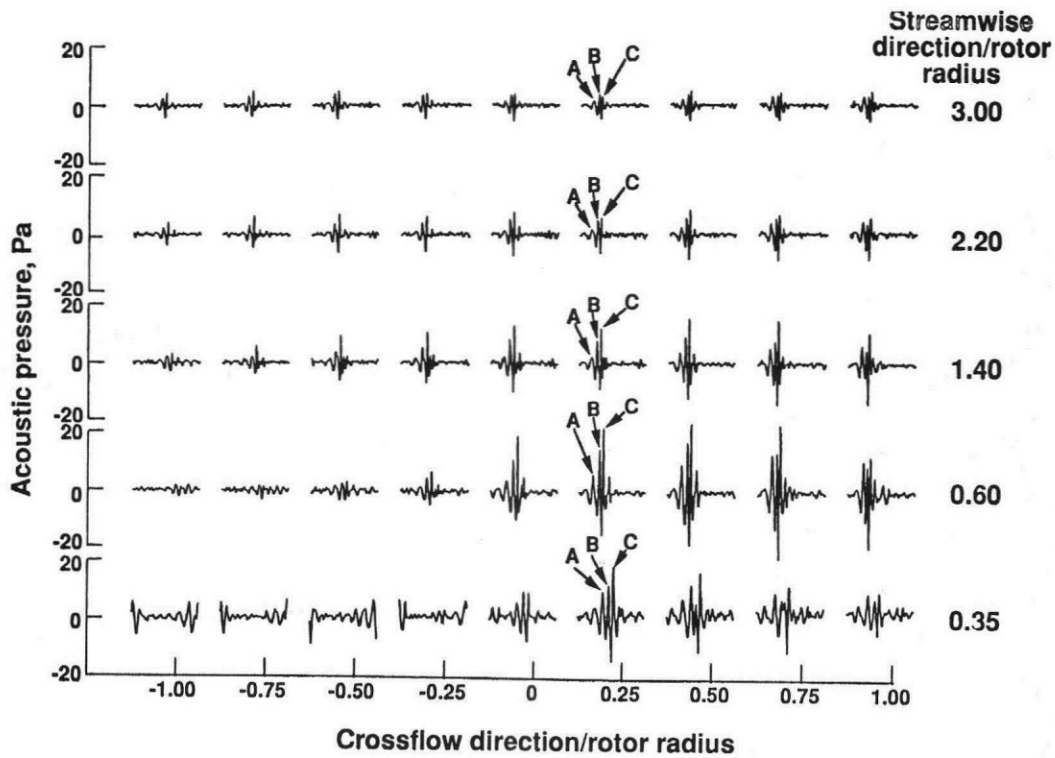


Figure 6. BVI time histories showing multiple impulses A, B, and C. $\mu=0.115$; $\alpha_{\text{TPP}}=3.4^\circ$.

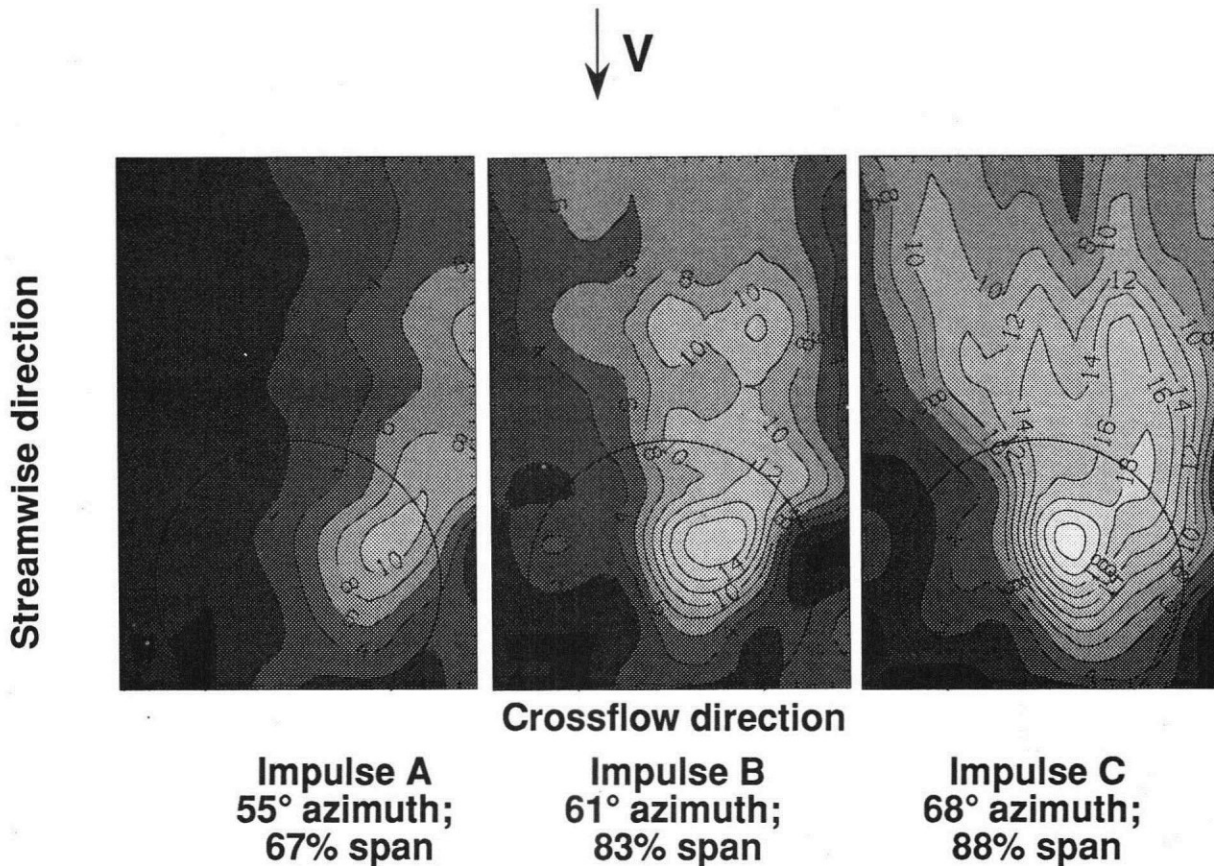


Figure 7. Directivity of peak values for impulses A, B, and C.

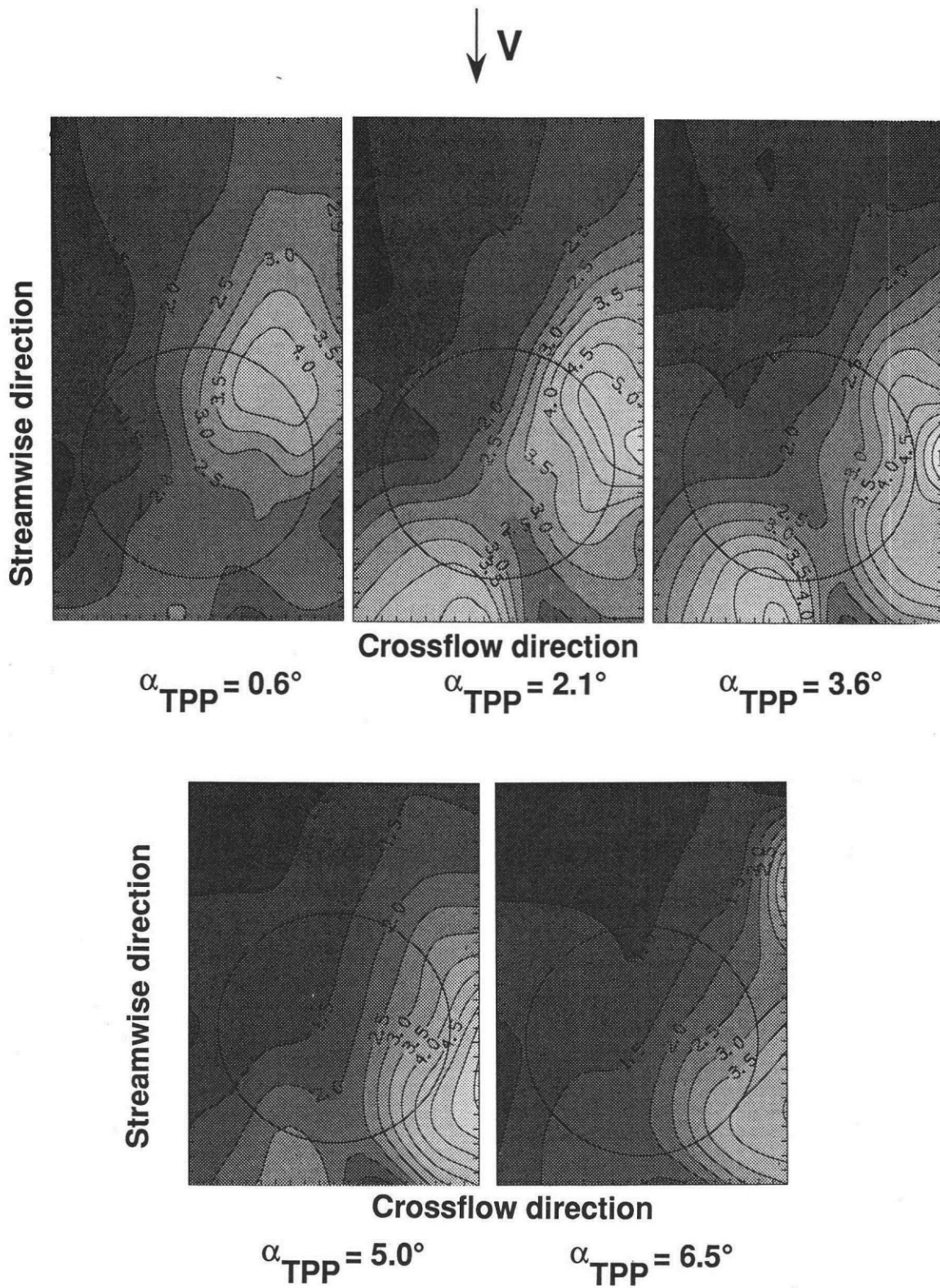


Figure 8. Variation of rms filtered BVI noise directivity with tip path plane angle. $\mu=0.15$.

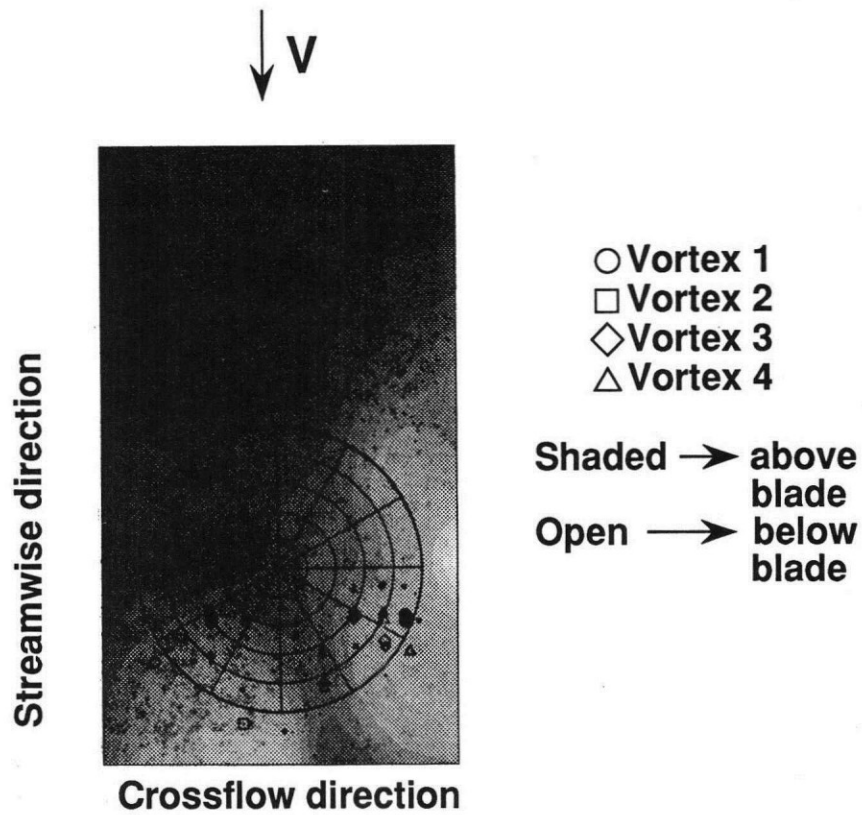


Figure 9. Predicted BVI regions. $\mu=0.15$; $\alpha_{TTP}=3.6^\circ$.

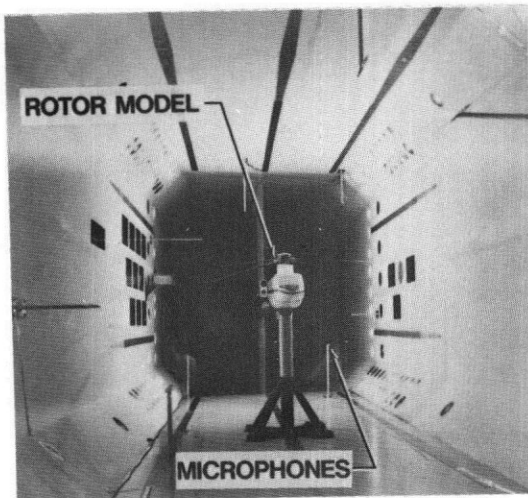


Figure 10. Photo of model rotor in TDT. Arrows show microphones of interest.

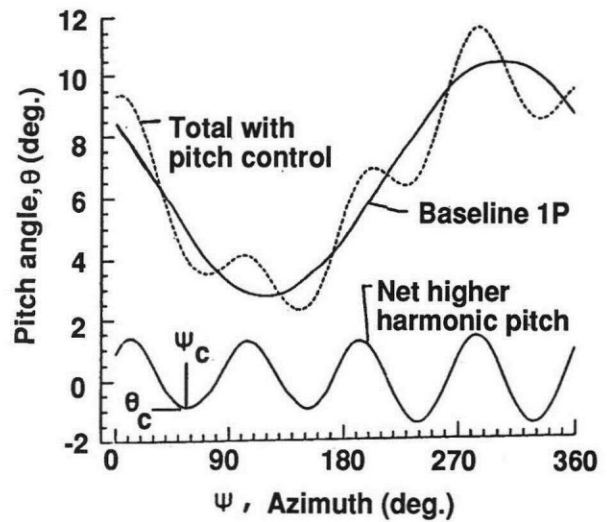


Figure 11. Blade pitch angle θ versus azimuth angle ψ for $\mu=0.266$ and $\alpha=0^\circ$. Pitch control is 4P collective with $\theta_c=-1.0^\circ$ and $\psi_c=60^\circ$.

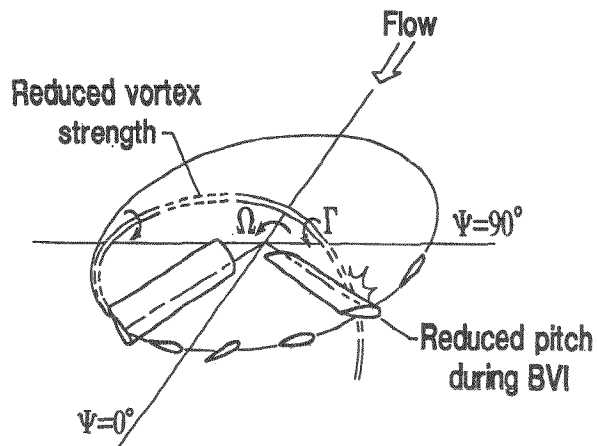


Figure 12. Illustration of noise reduction concept.

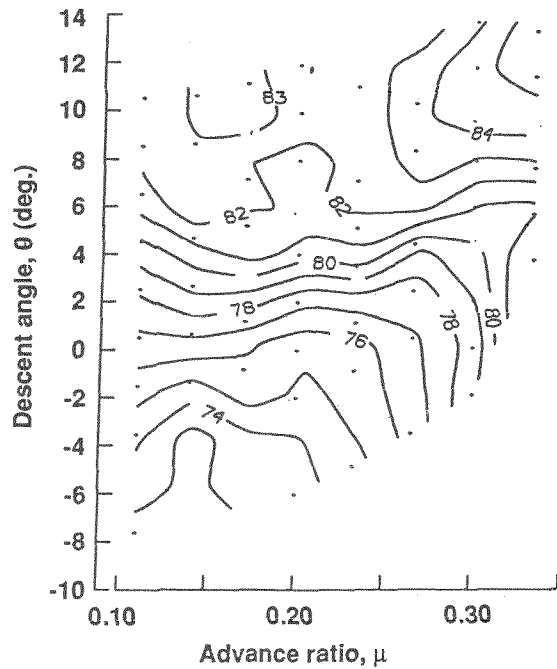


Figure 14. Noise level (dB) contours for different flight conditions for the 4P pitch control case. $\theta_c = -1.0^\circ$; $\psi_c = 60^\circ$.

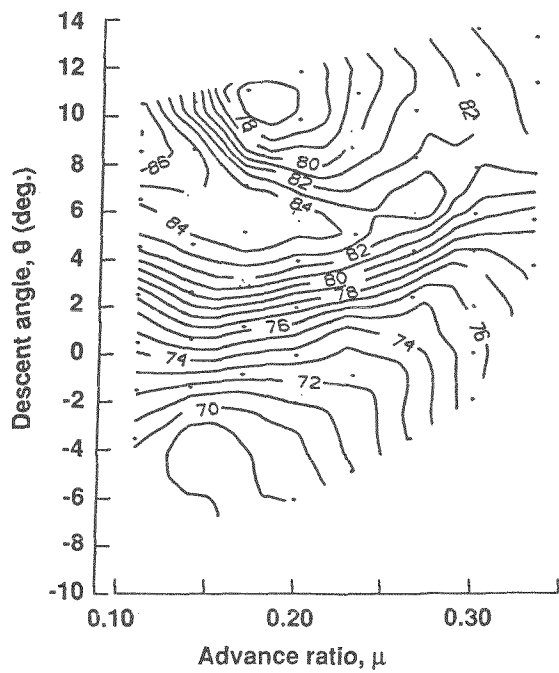


Figure 13. Noise level (dB) contours for different flight conditions for the baseline (no control) case.

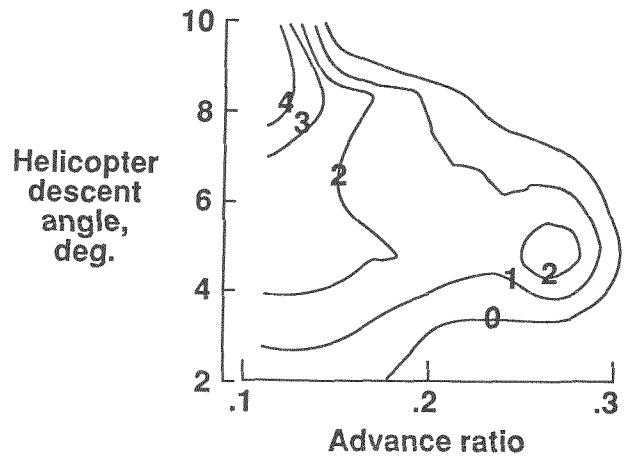


Figure 15. Noise reduction due to HHC.